EPJ manuscript No.
(will be inserted by the editor)

Open-Charm results on gluon polarisation from COMPASS

Celso Franco[1,a], on behalf of the COMPASS collaboration

LIP-Lisboa

Abstract. The gluon polarisation in the nucleon has been determined by detecting open-charm production in photon-gluon fusion processes. The data were taken by the COMPASS Collaboration at CERN between 2002 and 2006, colliding a polarised muon beam on a polarised deuteron target. At leading order QCD, an average gluon polarisation of $\langle \Delta g/g \rangle_x = -0.49 \pm 0.27(stat) \pm 0.11(syst)$ at a scale $\mu^2 \approx 13\ (GeV/c)^2$, and at an average gluon momentum fraction $\langle x \rangle \approx 0.11$, was estimated.

1 Introduction

Pioneering experiments on the nucleon spin structure (SLAC [1] and EMC [2]), obtained an unexpected small quark contribution to the proton spin:

$$\Delta\Sigma \approx 0.12 \pm 0.17 \tag{1}$$

Where $\Delta\Sigma$ is the first moment of the sum of the quark helicity distributions.
Theoretically one would naively expect, from the static quark model wave function, that *up* and *down* quarks carry all the nucleon spin *($\Delta\Sigma = \Delta u + \Delta d = 1$)*:

$$\mid p\uparrow \rangle = \frac{1}{\sqrt{18}}\{2 \mid u\uparrow u\uparrow d\downarrow \rangle - \mid u\uparrow u\downarrow d\uparrow \rangle - \mid u\downarrow u\uparrow d\uparrow \rangle + (u \leftrightarrow d)\} \tag{2}$$

$$\Delta u = \langle\ p\uparrow \mid N_{u\uparrow} - N_{u\downarrow} \mid p\uparrow \rangle = \frac{3}{18}(10-2) = \frac{4}{3} \tag{3}$$

$$\Delta d = \langle\ p\uparrow \mid N_{d\uparrow} - N_{d\downarrow} \mid p\uparrow \rangle = \frac{3}{18}(2-4) = -\frac{1}{3} \tag{4}$$

However if we apply relativistic corrections to the model *(like MITBag model)*, or assuming $SU(3)$ symmetry, a $\Delta\Sigma \approx 0.6$ is expected. This is still a large discrepancy between prediction and experiment, giving rise to the so called **spin crisis**. This fact triggered extensive studies on the nucleon spin structure in lepton scattering experiments at CERN by SMC [3] and COMPASS [4], at SLAC [5], DESY [6], JLAB [7], and also in polarised proton-proton collisions at RHIC [8, 9]. The results confirmed a small contribution from quarks to the nucleon spin with a very good precision *(see Ref. [4])*:

$$\Delta\Sigma = 0.30 \pm 0.02 \pm 0.01 \quad (world\ data\ at\ Q^2 = 3\ (GeV/c)^2) \tag{5}$$

Since we know that the nucleon spin must sum to 1/2, the problem was how to solve this **spin puzzle**. Taking into account orbital angular momenta, L, of quarks and gluons, the nucleon spin projection *(in units of $\hbar$)* can be decomposed into a sum of it's constituents:

[a] e-mail: celso@lip.pt

$$S_z = \frac{1}{2} = \frac{1}{2}\Delta\Sigma + \Delta G + L_z \tag{6}$$

The first guess to solve this spin puzzle is that the remaining part of the nucleon spin comes from the gluons *(ΔG is the first moment of the gluon helicity distribution)*. It is a reasonable assumption, since we know from the past that gluons were the solution to the so called momentum crisis in the nucleon *(gluons carry $\approx 1/2$ of the proton momentum)*.
This was a strong motivation for measuring the gluon contribution to the nucleon spin. Another motivation relies on the fact that in QCD, the U(1) anomaly, generates a contribution from gluons to the measured singlet axial coupling $a_0(Q^2)$. This implies that $\Delta\Sigma(Q^2)$ is scheme dependent and may differ from the observable $a_0(Q^2)$, while ΔG is scheme independent at least up to NLO. In the Adler-Bardeen scheme [10], $\Delta\Sigma^{AB}$ is independent of Q^2 *(which is suited for the Ellis-Jaffe prediction)*, and is related to the minimum subtraction scheme *($\overline{MS}$ scheme)* through the following equation:

$$\Delta\Sigma^{\overline{MS}}(Q^2) = a_0(Q^2) = \Delta\Sigma^{AB} - n_f\frac{\alpha_S(Q^2)}{2\pi}\Delta G(Q^2) \tag{7}$$

Assuming the Ellis-Jaffe prediction of $\Delta\Sigma^{AB} \approx 0.6$, this requires values of $\Delta G(Q^2) \approx 2$ *and* $L_z \approx -2$ *(at* $Q^2 = 5\ (GeV/c)^2$*)*, in order to be compatible with $a_0 \approx 0.3$.
Due to a limited range in Q^2 covered by the polarised experiments, the QCD analysis *(through the evolution of DGLAP equations)* shows a limited sensitivity to the gluon helicity distribution *(as a function of the gluon momentum fraction x)*, $\Delta g(x)$, and to its first moment, ΔG. The determination of $\Delta g(x)$ from QCD evolution must then be complemented by direct measurements in dedicated experiments like COMPASS.

2 The COMPASS Experiment

COMPASS is a fixed target experiment at the M2 muon beam line of the CERN SPS. Since its main purpose is to study nucleon spin, a polarised beam colliding in a polarised target is mandatory.
The muon beam is naturally polarised, with an average polarisation in laboratory of about 80% at 160 GeV/c. This polarisation is achieved in an elegant way, resulting from parity violation decays of π^+ *($\approx 98\%$ of the cases)* and K^+, which are produced by collisions of the SPS proton beam on a thick absorber. In the rest frame of pion, this polarisation is 100% due to the natural helicity of neutrinos involved *(pions have $\approx$ 600 m to decay)*:

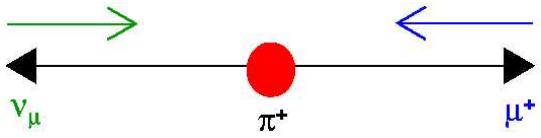

Fig. 1. Naturally polarised beam production

The polarised target consists of ^6LiD beals housed in a superconducting solenoid. The polar angle acceptance to the spectrometer goes up to 70 mrad for data taken in 2002-2004, and to 180 mrad for 2006 year. This upgrade was of crucial importance to increase the statistics available for this analysis *(more slow particles detected at larger angles)*. The target material is divided in two 60-cm-long cells, longitudinally polarised in opposite directions. The spin directions were reversed every eight hours, by rotating the field of the target magnet system, in order to minimize effects resulting from the acceptance difference between the 2 cells. In 2006 a 3-cell target configuration was used in order to reduce systematic errors related to different acceptances. A central 60-cm-long cell is placed between two 30-cm-long cells with

polarisations opposite to the central one. In this way, a similar average acceptance between the two spin configurations is obtained, and the magnetic field was rotated only once per day. The average target polarisation is, $P_t \approx 50\%$, with a dilution factor $f \approx 0.4$ *(which accounts for the fraction of polarisable material).*
The particles produced in these DIS collisions are then detected in a two stage spectrometer, whose detailed description can be found in *Ref. [11].* Basically this two parts are defined by two large magnets, with several tracking devices in each of them. The first part is the large angle spectrometer, dedicated to low momentum tracks reconstruction, while the second part was designed to smaller angles detection:

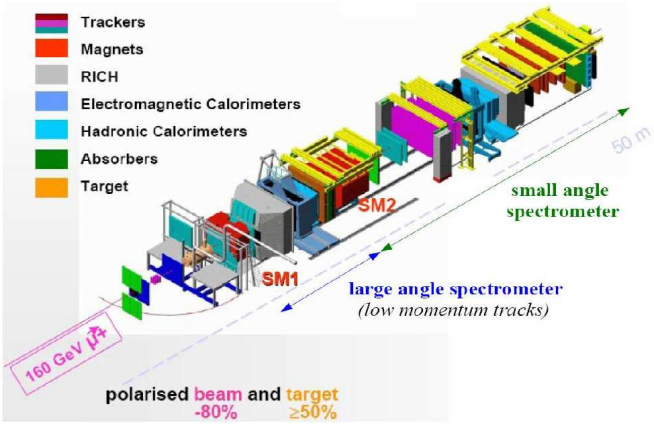

Fig. 2. COMPASS spectrometer

A Ring Imaging CHerenkov (RICH) detector, with C_4F_{10} as radiator gas, is used in the first spectrometer for charged particle identification *(of crucial importance for this analysis).* It consists of several multi-wire proportional chambers, with CsI photocathodes, which detect the UV components of the Cherenkov light. In 2006 there was a considerable upgrade, with the central part of the detector replaced by multi-anode photomultiplier tubes, yielding a larger number of photons detected *(extending the range of detection to the visible wavelength)* together with a much faster response *(reducing the uncorrelated background of halo muons).* Together with a readout electronics refurbishment, this allowed a much cleaner particle identification.

3 Open-charm events selection

In the present analysis D^0 and D^* mesons are used. In order to be sensitive to the gluon polarisation inside the nucleon, we must tag a process involving a polarised lepton-gluon interaction producing these open-charm events *(see Fig. 3).* To achieve this we need to reconstruct the incoming and outgoing muon, the interaction vertex inside the polarised target, and at least two additional tracks. D^0 mesons are reconstructed *(only one per event)* through the invariant mass calculation of their decay products, since the multiple Coulomb scattering of charged particles in the solid state target does not allow good spatial resolution in vertex reconstruction. The following decay channels are considered:

$$D^0 \to K^-\pi^+ \quad and \quad \bar{D}^0 \to K^+\pi^- \quad (with\ a\ branching\ ratio\ of\ 3.9\%) \tag{8}$$

$$D^{*+} \to D^0\pi^+_{slow} \quad and \quad D^{*-} \to \bar{D}^0\pi^-_{slow} \quad (\approx\ 30\%\ of\ total\ D^0\ sample) \tag{9}$$

In order to reduce the large combinatorial background from the nucleon fragmentation, only identified $K\pi$ pairs are used. A likelihood for different mass hypotheses and background hypotheses is computed *(likelihood functions are defined from the expected angular distribution of*

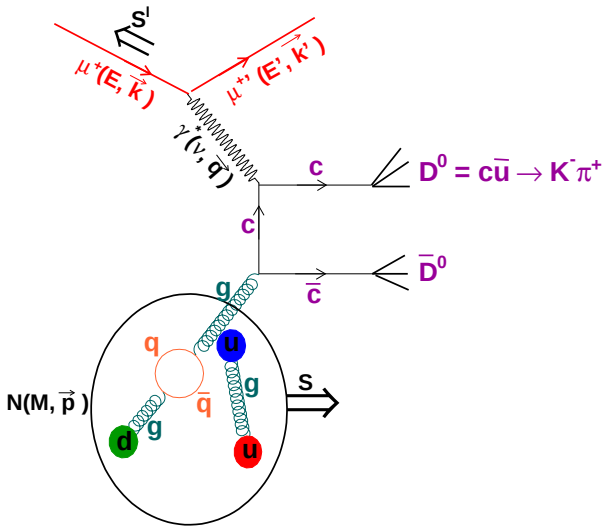

Fig. 3. Open-Charm production in polarised photon-gluon fusion process

Cherenkov photons), for particles entering the RICH detector with measured momenta. This is done for each track using the angles between the track and the detected Cherenkov photons. For background, a sample of photons not associated to reconstructed tracks was used. Particles are identified as kaons or pions, if the likelihood for the corresponding mass hypotheses is higher than all the others. In the case of D^* channel an additional slow pion is present. Likelihoods are used to reject electrons that could be misidentified as this extra particle, reducing the combinatorial background by a factor of 2.
Some kinematic cuts are applied, in the fraction of the virtual photon energy carried by the D^0, $z_{D^0} > 0.2/0.25$ *(for D^*/D^0)*, and in the angle of kaon decay in D^0 center-of-mass, $|cos(\theta^*)| < 0.9/0.65$ *(for D^*/D^0)*. This avoids more combinatorial background since events coming from the fragmentation of the struck quark, from LO processes, are collinear to the virtual photon direction, and with a z_{D^0} close to zero. Final samples are shown in *Fig. 4*, with 8700 D^* and 37400 D^0 reconstructed in this way *(In D^* channel what is actually reconstructed is the D^0, so from now on D^* should be interpreted as a D^0 tagged with a D^*)*.
The D^* sample is very clean because it is a 3-body decay, and an additional cut on the reconstructed D^* and D^0 mass differences is applied:

$$3.2\ MeV/c^2 < M_{D^*} - M_{D^0} - M_\pi < 8.9\ MeV/c^2 \tag{10}$$

We see that there is not much space left for slow pion momenta, resulting in a good peak resolution. In D^* channel there is also a bump in mass distribution at $\approx -250\ MeV/c^2$, because there is one mode of D^0 decay involving an extra π^0 which is not considered in this analysis. In D^0 spectra this is not seen due to a larger combinatorial background. Events present in D^* sample are not allowed to be present in D^0 sample.

3.1 Why open-charm?

This channel is ideal for probing gluon polarisation because $c\bar{c}$ production is dominated by the photon-gluon fusion process *(PGF)*, in the COMPASS center of mass energy. Also according to the intrinsic charm *(c quarks not comming from hard gluons)* models available, we can say that this process is free from physical background. This can be seen qualitatively in *Fig. 5*, where the reconstructed and generated *(for PGF process)* z_{D^0} variable is shown. For PGF it is

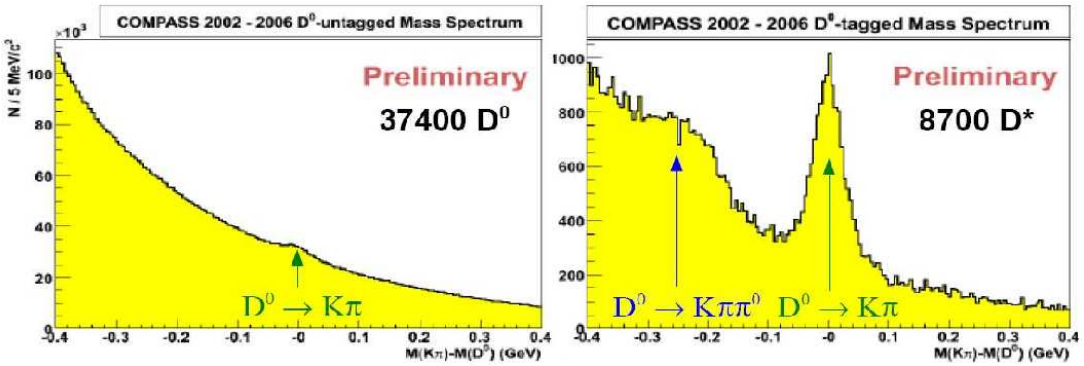

Fig. 4. D^0 and D^* invariant mass spectra

expected that this distribution peak arround 0.5, since each c quark recieves roughly the same amount of γ^* energy. If the nucleon intrinsic charm is not negligible, the distribution should peak towards one.
In *Fig. 6* one can see that the predicted intrinsic charm contamination in COMPASS kinematic domain is negligible. Experimental points represent measurements of charm structure function by EMC experiment [12], at COMPASS energy ν, and black dotted curves reveals the theoretical distribution for PGF with different renormalization and factorization scales. Blue curve shows intrinsic charm prediction assuming nucleon fluctuation into charmed meson-hadron pairs *(see Ref. [13])*, and red dashed curve shows intrinsic charm prediction assuming charm fluctuations at partonic level *(as in Ref. [14])*.
Also the resolved photon contribution to open-charm production via gluon-gluon fusion was estimated with RAPGAP generator [21], and can be neglected in the kinematic range of the present analysis.
From this one can conclude that this channel is ideally suited for direct measurement of gluon polarisation, because it is free from physical background. However, the weakness of this method is its poor statistical significance.

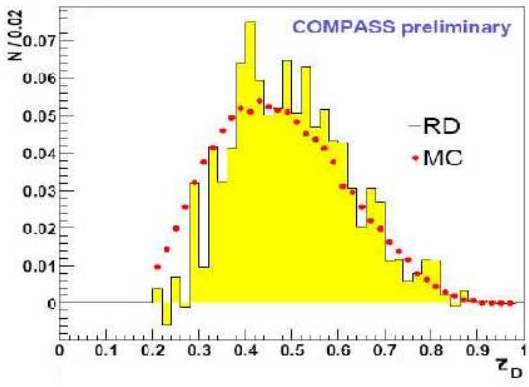

Fig. 5. Reconstructed vs. generated virtual photon energy fraction carried by the D^0 meson *(2003 data)*

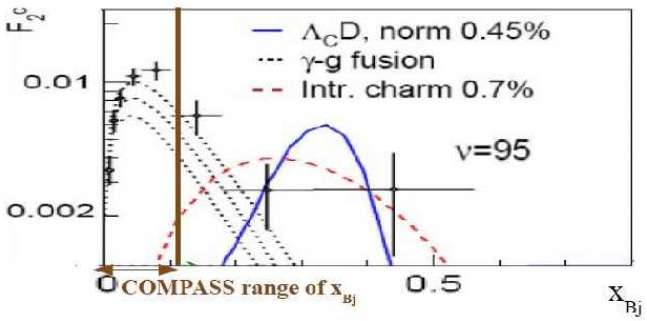

Fig. 6. Nucleon intrinsic charm models

4 Method for gluon polarisation extraction

To access the gluon polarization, we measure the asymmetry in the number of open-charm events reconstructed inside each target cell:

$$A^{exp} = \frac{n^u - n^d}{n^u + n^d} = f P_\mu P_t A^{\mu,N} + A^{bg} \tag{11}$$

with:

$$A^{\mu,N} = DA_1 = D\frac{\sigma^{\rightarrow\leftarrow}_{\gamma,N} - \sigma^{\rightarrow\rightarrow}_{\gamma,N}}{\sigma^{\rightarrow\leftarrow}_{\gamma,N} + \sigma^{\rightarrow\rightarrow}_{\gamma,N}} = D(\frac{\Delta\sigma}{\sigma})^{\gamma N \to c\bar{c}X} \tag{12}$$

The number of events inside first cell are defined as n^u, with n^d coming from the second cell polarised in opposite direction:

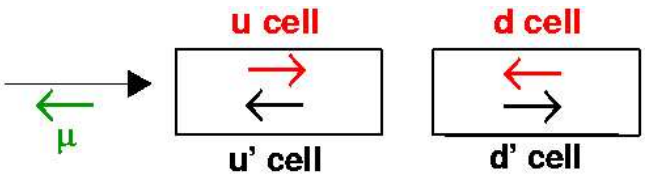

Fig. 7. Target scheme *(2002-2004 data)*

This experimental asymmetry is proportional to the muon-nucleon asymmetry, taking into consideration some experimental factors *(dilution factor f, beam polarisation P_μ, and target polarisation P_t)*. Also a second term involving the contribution of polarised background must be taken into account. $A^{\mu,N}$ is related to the photon-nucleon cross section asymmetry, A_1, through the depolarisation factor, D, which accounts for the polarisation transfer from the lepton to the virtual photon [15].
In the quark-parton model interpretation, the photon-nucleon asymmetry is defined as the ratio of polarised and unpolarised nucleon structure functions *($A_1 = g_1/F_1$)*. Using this asymmetries one can study the nucleon spin, and the advantage of measuring asymmetries with respect to cross-section differences is that for the second we have to measure the overall experimental acceptance, the efficiency, and the total incoming flux. Moreover, the effects of changes in the experimental conditions have stronger impact on the precision of the data.
Eq. 11 can be redefined in terms of number of open-charm events:

$$\frac{dn}{dmdX} = a\phi\eta(s+b)[1 + P_t P_\mu f(\frac{s}{s+b}A_S + \frac{b}{s+b}A_B)] \tag{13}$$

With $m = M_{K\pi}$, X represents a set of kinematic variables ($Q^2, Z_{D^0}...$) defining the event, a is the spectrometer acceptance, ϕ is the integrated muon beam flux, and η the number of target nucleons. *s/s+b* is the signal purity with signal events, s(m, X), coming from the invariant mass spectra peak. s(m, X) and b(m, X) represent the differential unpolarised cross section of signal and background events folded with the experimental resolution.
In LO QCD, A_S can be defined as a convolution between the partonic polarised/unpolarised cross section *(for the process $\mu g \to \mu' c\bar{c}$)*, with the polarised/unpolarised gluon structure function *($\Delta g/g$)*:

$$A_S(X) = A^{\mu,N} = A_1(X)D = \frac{\int \Delta\hat{\sigma}\Delta g F dY}{\int \hat{\sigma} g F dY} = a_{LL}(X)\frac{\Delta g}{g}(X) \tag{14}$$

where:

$$a_{LL}(X) = \frac{\int \hat{a}_{LL}\hat{\sigma} g F dY}{\int \hat{\sigma} g F dY} \quad (\textit{with partonic asymmetry } \hat{a}_{LL} = (\frac{\Delta\hat{\sigma}}{\hat{\sigma}})^{\mu' g \to \mu' c\bar{c}}) \tag{15}$$

$$\frac{\Delta g}{g}(X) = \frac{\int a_{LL}\hat{\sigma} g F \frac{\Delta g}{g} dY}{\int a_{LL}\hat{\sigma} g F dY} \tag{16}$$

F describes the fragmentation of c quarks into D^0 mesons, and the integration is done over partonic variables, Y, not accessible from the event kinematics, like for example the gluon momentum fraction x_g.
Since the factors *s/s+b* and a_{LL} have a large dispersion, a weighting method was used to reduce the statistical error. This is also more correct since events with low factors carry less information about the asymmetry. All events are weighted with the following signal and background weights:

$$\omega_S = P_\mu f a_{LL}\frac{s}{s+b} \tag{17}$$

$$\omega_B = P_\mu f D\frac{b}{s+b} \tag{18}$$

With this definitions the statistical error is minimized *(see ref. [4])*. The target polarisation is not included in the weight because it is a time dependent quantity, and because of this it may generate false asymmetries. As a result of this weighted method, events with a poor signal purity do not have to be removed by a more tight kinematic cut.
From *Fig. 7* one can see that we have 2 cells with opposite polarisations. However, in order to minimize acceptance effects between cells, target spins where reversed every eight hours. As a result we end up with 2 cells with 4 possible configurations *(for 2006 data we still consider 2 cells by summing first and last cell events)*, t = u, d, u', d'. We can define 4 equations from *eq. 13*, for the number of events, and by weighting them with a signal weight and then with a background weight we end up with 8 equations and 10 unknowns *($\langle\Delta g/g\rangle_x, A_B$, and the 8 acceptance factors $\alpha_C^t = \int a^t\phi^t n^t(s+b)w_C dX$ with $C = S, B$)*:

$$\sum_{i=1}^{n_t} w_{C,i} = \alpha_C^t(1 + \beta_C^t\langle\frac{\Delta g}{g}\rangle_x + \gamma_C^t A_B) \tag{19}$$

with:

$$\beta_C^t = \frac{\sum_{i=1}^{n_t} P_{t,i}w_{S,i}w_{C,i}}{\sum_{i=1}^{n_t} w_{C,i}}, \quad \gamma_C^t = \frac{\sum_{i=1}^{n_t} P_{t,i}w_{B,i}w_{C,i}}{\sum_{i=1}^{n_t} w_{C,i}} \tag{20}$$

The only assumption we have here is that $\langle\Delta g/g\rangle_x$ and A_B are constant over the mass range considered, $-400\ MeV/c^2 < M_{K\pi} - M_{D^0} < 400 MeV/c^2$. Assuming that possible acceptance variations in time affect both cells in same way, the number of unknowns is reduced to 8:

$$\frac{\alpha_C^u}{\alpha_C^d} = \frac{\alpha_C^{u'}}{\alpha_C^{d'}} \tag{21}$$

With a much weaker assumption, that signal and background events from same target cell are affected in the same way by the acceptance variations, the system is reduced to 7 unknowns:

$$\frac{\alpha_S^u}{\alpha_B^u} = \frac{\alpha_S^{u'}}{\alpha_B^{d'}} \quad and \quad \frac{\alpha_S^d}{\alpha_B^d} = \frac{\alpha_S^{d'}}{\alpha_B^{d'}} \tag{22}$$

After this constraints, the system can be solved by a χ^2 minimization *(***f** *corresponds to a vector containing the 8 functions of eq. 19)*:

$$\chi^2 = (\mathbf{n} - \mathbf{f})^T Cov^{-1} (\mathbf{n} - \mathbf{f}) \tag{23}$$

However to solve this system of 8 equations with 7 unknowns, we still need to have a_{LL}, *s/s+b*, f, P_t, P_μ, and D for every event. P_μ is parameterized as a function of the incoming muon momentum, P_t is averaged over one hour of data taking, and f is calculated as in *Ref. [16].*
The partonic asymmetry, $a_{LL}(X)$, is parameterized *(as* $a_{LL}(X)/D$*)* in terms of measured kinematic variables. Since only one D^0 meson is reconstructed in each event, we don't have access to all partonic variables on which this asymmetry depends. To solve this, leading order PGF events were generated with AROMA [17], and then processed by GEANT to simulate the response of the spectrometer. Finally they were reconstructed like real events, serving as input for a Neural Network parameterization on the reconstructed event kinematics. The correlation between generated and parameterised a_{LL} is 82%, and can be seen in *Fig. 8.* For the generation a scale, μ, was chosen as the transverse mass of the produced charm quark pair, and is large enough to justify the perturbative approach.

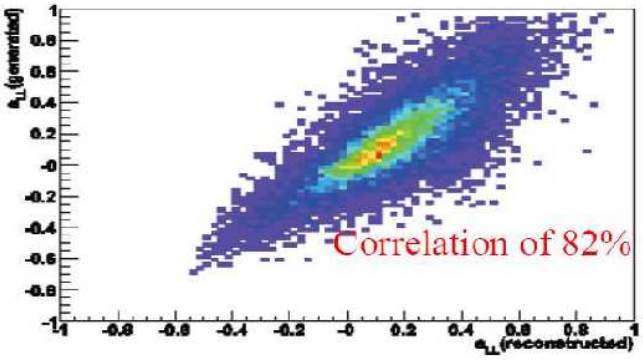

Fig. 8. Correlation between reconstructed and generated partonic asymmetry a_{LL}

The last factor missing is the signal purity, *s/s+b*, which was parameterised for every event as a function of the relevant kinematic variables and RICH response. The invariant mass spectra is divided in bins *(typically 6)* for 10 variables, to take into account other dependences in *s/s+b* than the mass. Inside this bins, for each variable, the invariant mass distribution is fitted with a gaussian to account for the signal. For background, a sum of an exponential with a gaussian is used for D^*, and two exponentials for D^0 channel. A function is then defined for each variable *(to build* $\Sigma_p = (s/b)_p$*)*, and adjusted to the s/b ratios from the fit inside each bin *(in a mass window of* $\pm 40/30\ MeV/c^2$ *(*D^*/D^0*) around the peak).* Each variable is taken successively, with the parameterisation defined as the product of this 10 functions. The procedure continues in a iterative way until convergence inside bins of all variables is reached *(parameterised function is*

reproducing simultaneously s/b ratios from fit). Finally the signal purity is obtained from a fit to the mass spectra in bins of $\Sigma = s/s+b = \Sigma_p/(1+\Sigma_p)$ *(for D^0 and D^* separately).* This value is then adjusted to match the exact value of Σ_p for each event of a particular Σ bin *(note that events are properly sorted inside this bins, reflecting the same dependences on kinematics and RICH response, and thus reducing the statistical error [because clean peaks introduce bigger weights, as in Fig. 9]):*

$$\frac{s}{s+b} = \frac{\lambda s(m)}{\lambda s(m) + b(m)} \quad with\ \lambda = \Sigma_p \div \frac{\int_{-3\sigma}^{+3\sigma} s(m)}{\int_{-3\sigma}^{+3\sigma} b(m)} \tag{24}$$

This parameterisation was tested on a wrong charge background, $K^-\pi^+\pi^-_{slow}$, and no artificial peak was generated at $M_{K\pi} = M_{D^0}$, leading to a consistent result. Parameterised $s/s+b$ acts like a probability for each event *(from all spectra)* to be a signal, allowing events with poor signal purity to contribute also to the statistics. This probability effect can be checked in *Fig. 9* for D^* channel, where values of $s/s+b$ near unity are more likely to be signal. The mean value of this parameterisation around the peak, inside this probability bins, matches signal purity from the fit *(meaning that no bias is introduced).*

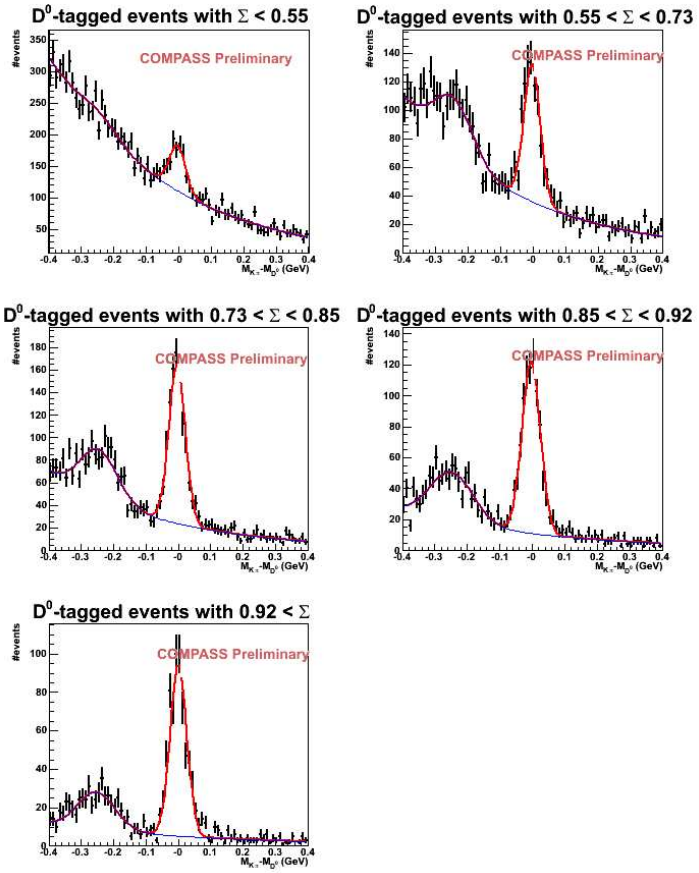

Fig. 9. D^* invariant mass spectra in signal probability bins

5 Results

Using the method described above, a value for $\langle \Delta g/g \rangle_x$ was obtained for each of the 40 weeks of data *(to minimize statistical error)*, for each channel separately. Since $\Delta g/g(x)$ is linearly dependent on x in the range covered, we end up with a measurement of $\Delta g/g(\langle x \rangle)$ *(where* $\langle x \rangle$ *is calculated using the signal weights)*. Results for each year and channel, for $\Delta g/g(\langle x \rangle)$, can be seen on *Fig. 10*. The final value is the weighted mean of these results and has the value of:

$$\langle \frac{\Delta g}{g} \rangle_x = -0.49 \pm 0.27(stat) \pm 0.11(syst) \tag{25}$$

A_B was extracted simultaneously and found to be consistent with zero.

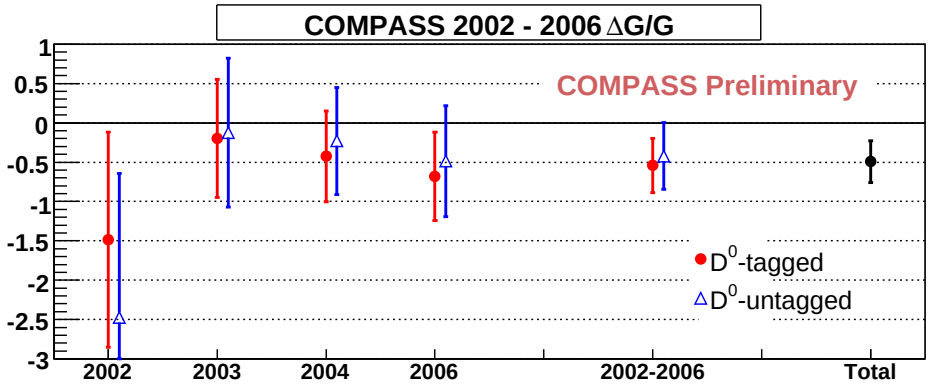

Fig. 10. $\langle \Delta g/g \rangle_x$ as a function of data taking year *(D^* and D^0)*

5.1 Systematic errors

The systematic error associated with this measurement of $\langle \Delta g/g \rangle_x$ is 0.11, whose main sources can be found on *table 1*. The origin of the contribution of P_μ, P_t and f, to the systematic error can be found on *Ref. [4]*. Concerning false asymmetries, data samples were divided into two in order to check consistency. For example, $D^{0's}$ going to the left or to the right in the spectrometer, gives values of the asymmetries which are compatible within the errors. Also the target stability was checked, by dividing data in two parts coming from different target positions. From all this studies, no false asymmetries were observed.
We know also that possible errors on the weights result in an error which is proportional to $\Delta g/g$. A conservative value of 0.05 was obtained according to *Ref. [4]*, using the dispersion of the 40 $\langle \Delta g/g \rangle_x$ and A_B values.
Concerning signal purity, it was obtained in different mass windows, different fit functions were used, different order for the parameterised variables was tried, as well as for different number of iterations. For a_{LL} generaion, different masses for the charm quark and different parton distribution functions were used.
Using this information, for a nominal analysis with weight w^0, and uncertainty in the weight w^i *(which are the different approaches defined above)*, the spread in $\langle \Delta g/g \rangle_x$ is given by the spread of:

$$\frac{\langle \omega^0 \omega^i \rangle}{\langle (\omega^0)^2 \rangle} \tag{26}$$

As a final comment, the much larger value obtained for the systematic error of the D^0 sample *(0.07 compared with 0.01 of D^*)* in *s/s+b*, is intuitively justified by the much lower signal purity in this channel.

Source	D^0	D^*
Beam polarisation	0.025	0.025
Target polarisation	0.025	0.025
Dilution factor	0.025	0.025
False asymmetry	0.05	0.05
$\frac{s}{s+b}$	0.07	0.01
a_{LL}	0.05	0.03
Total	0.11	0.07

Table 1. Systematic error contribution

6 Conclusion

A direct measurement of $\langle \Delta g/g \rangle_x$ was performed from the asymmetry on D^0 meson production, with a statistical precision of 0.27. The systematic contribution of 0.11 is negligible as compared to the statistical error. The result was obtained in LO QCD, for PGF process, and it can be compared with COMPASS high-pt hadron pairs method and results from other experiments in *Fig. 11.* Curves shown represent parameterisations from the COMPASS QCD analysis of the structure function data *(Ref. [4])*. The open-charm point is consistent with other measurements, favouring small values of $\langle \Delta g/g \rangle_x$. However, the scale of this analysis is $\mu^2 \approx 13(GeV/c)^2$, while all other points and curves are at a scale $\mu^2 \approx 3(GeV/c)^2$.
In this analysis the result shown is weak model dependent *(Monte-Carlo)*.

References

[1] V.W. Hughes, Nucl. Phys. A **518** (1990) 371
[2] EMC, J. Ashman *(et all.,)* Nucl. Phys. B **206** (1988) 364
[3] SMC, B. Adeva *(et all.,)* Phys. Rev. D **58** (1998) 112001
[4] COMPASS, V. Yu. Alexakhin *(et all.,)* Phys. Lett. B **647** (2007) 8
[5] E155, P. L. Anthony *(et all.,)* Phys. Lett. B **463** (1999) 339
[6] Hermes, A. Airapetian *(et all.,)* Phys. Rev. D **75** (2007) 012007
[7] CLAS, K. V. Dharmawardane *(et all.,)* Phys. Lett. B **641** (2006) 11
[8] PHENIX, A. Adare *(et all.,)* Phys. Rev. D **76** (2007) 051106(R)
[9] STAR, B. I. Abelev *(et all.,)* Phys. Rev. D **97** (2006) 252001
[10] R. D. Ball, S. Forte and G. Ridolfi, Phys. Lett. B **378** (1996) 255
[11] COMPASS, P. Abbon, *(et all.,)* Nucl. Instr. Meth. A. **577** (2007) 455
[12] EMC, J J Aubert, *(et all.,)* Nucl. Phys. B **213** (1983) 31 and hep-ph/9508403
[13] hep-ph/0508126
[14] S.J. Brodsky, *(et all.,)* Phys. Lett. B **93** (1980) 451
[15] COMPASS, V. Yu. Alexakhin *(et all.,)* Phys. Lett. B **647** (2007) 330
[16] COMPASS, E. S. Ageev *(et all.,)* Phys. Lett. B **612** (2005) 154
[17] G. Ingelman, *(et all.,)* Comput. Phys. Commun. **101** (1997) 135
[18] COMPASS, E. S. Ageev *(et all.,)* Phys. Lett. B **633** (2006) 25
[19] SMC, B. Adeva *(et all.,)* Phys. Rev. D **70** (2004) 012002
[20] HERMES, A. Airapetian *(et all.,)* Phys. Rev. Lett. D **84** (2000) 2584
[21] H. Jung. Comput. Phys. Commun. **86** (1995) 147

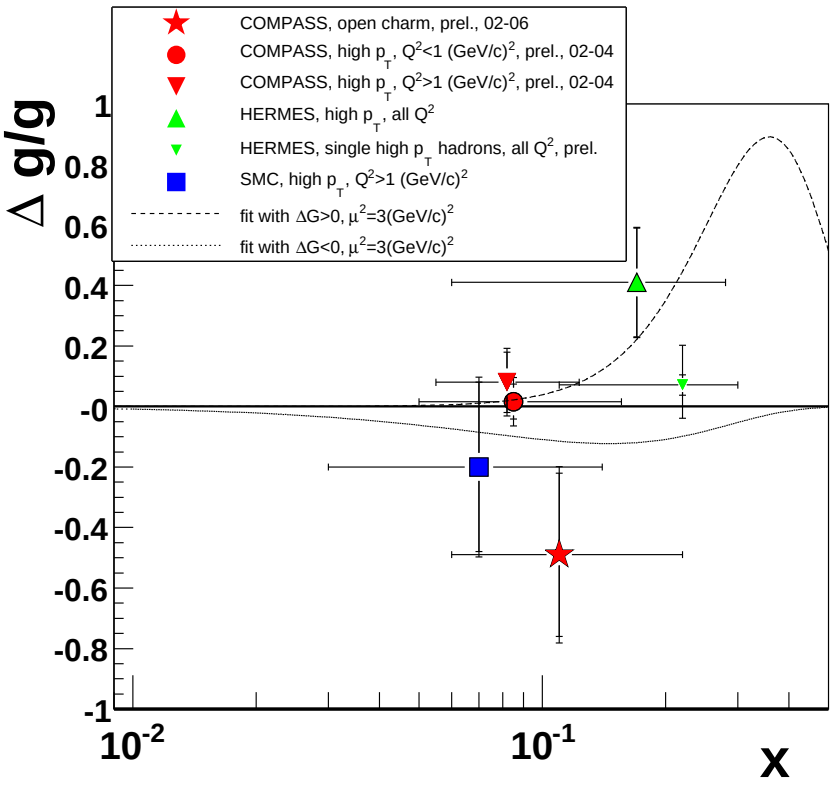

Fig. 11. Compilation of the $\langle \Delta g/g \rangle_x$ measurements from open-charm and high p_T hadron pair production by COMPASS [18], SMC [19] and HERMES [20] as a function of x. The horizontal bars mark the range in x for each measurement, the vertical ones give the statistical precision and the total errors *(if available)*. The open-charm measurement is at a scale of about $13(GeV/c)^2$, other measurements at $3(GeV/c)^2$. The curves display two parameterisations from COMPASS QCD analysis at NLO [4], with $\Delta G > 0$ *(broken line)* and with $\Delta G < 0$ *(dotted line)*

.